RSC Advances

PAPER

View Article Online
View Journal | View Issue

Cite this: *RSC Adv.*, 2020, **10**, 21830

Synthesis and molecular modeling studies of cholinesterase inhibitor dispiro[indoline-3,2′-pyrrolidine-3′,3″-pyrrolidines]†

M. Adel Youssef,[a] Siva S. Panda,[b] Riham A. El-Shiekh,[c] ElSayed M. Shalaby,[d] Dalia R. Aboshouk,[e] Walid Fayad,[f] Nehmedo G. Fawzy[e] and Adel S. Girgis *[e]

Received 5th April 2020
Accepted 29th May 2020

DOI: 10.1039/d0ra03064c

rsc.li/rsc-advances

A set of dispiro[indoline-3,2′-pyrrolidine-3′,3″-pyrrolidines] **8a–l** was regioselectively synthesized utilizing multi-component azomethine cycloaddition reaction of 3-(arylmethylidene)pyrrolidine-2,5-diones **5a–e**, isatins **6a–c** and sarcosine **7**. Single crystal X-ray studies of **8c** add conclusive support for the structure. Compounds **8e** and **8g** reveal cholinesterase inhibitory properties with promising efficacy against both AChE and BChE and were found to be more selective towards AChE than BChE as indicted by the selectivity index like Donepezil (a clinically used cholinesterase inhibitory drug). Molecular modeling studies assist in understanding the bio-observations and identifying the responsible parameters behind biological properties.

Introduction

Dementia is one of the most serious health problems for older people. About 50 million people are suffering from dementia globally with 10 million new cases yearly according to the WHO (World Health Organization).[1] Alzheimer's disease (AD) represents the most common cause of dementia (60–70%).[1] AD is a fatal chronic neurodegenerative disease associated with memory impairment and language deficits besides high degeneration of cholinergic neurons of the central nervous system.[2,3] Although no cure has been discovered for AD, a few pharmacological targets have been rationalized. Reduction of formation and aggregation of pathological hallmarks of AD (insoluble amyloid-β oligomers and tau neurofibrillary tangles) is a pharmacological target for AD. Other targets include modulation of neurotransmitter signals (cholinesterase inhibitors and *N*-methyl-D-aspartate receptor blockers).[4] Although the full mechanism of AD is not well elucidated yet, extensive studies explained that the brain of AD patients suffers from cholinergic neuron damage. This is why acetylcholine (AC) level is considered an important therapeutic target of AD. AC is an important brain neurotransmitter with major roles in memory and maintaining consciousness.[5] Acetylcholinesterase (AChE) is a catabolic enzyme capable for hydrolysis of AC. Butyrylcholinesterase (BChC) also regulates the AC levels. This is why inhibition of both cholinesterases is useful for AD patients.[2,6] Tacrine (Cognex) **1** was the first cholinesterase inhibitor approved drug[7] (Fig. 1). However, due to many clinically adverse effects including elevated liver transaminase levels it has been discontinued in many countries.[8,9] Meanwhile, many researchers are still interested in this compound for developing analogs of lesser side effects.[9–11]

Currently, many cholinesterase inhibitors are clinically used as AD drugs of which Galantamine (Razadyne) **2** (approved by FDA "Food and Drug Administration" on 28 Feb. 2001) for mild and moderate AD.[4,12,13] Rivastigmine (Exelon) **3** (approved by FDA in 21 April 2000) is also useful for mild and moderate dementia patients caused by AD or Parkinson's disease.[4,14,15] Donepezil (Aricept) **4** is also a cholinesterase inhibitor approved by FDA on 25 Nov. 1996 for AD.[4,16,17] Currently, available drugs are used to manage and prevent progress of the disease over time but unfortunately not able to cure. Additionally, the drugs lack long term efficacy and also associated with severe side

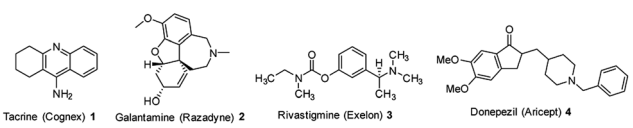

Fig. 1 Cholinesterase inhibitor drugs useful for AD.

[a]*Department of Chemistry, Faculty of Science, Helwan University, Helwan, Egypt*
[b]*Department of Chemistry and Physics, Augusta University, Augusta, GA 30912, USA*
[c]*Department of Pharmacognosy, Faculty of Pharmacy, Cairo University, Cairo 11562, Egypt*
[d]*X-Ray Crystallography Lab., Physics Division, National Research Centre, Dokki, Giza 12622, Egypt*
[e]*Department of Pesticide Chemistry, National Research Centre, Dokki, Giza 12622, Egypt. E-mail: girgisas10@yahoo.com*
[f]*Drug Bioassay-Cell Culture Laboratory, Pharmacognosy Department, National Research Centre, Dokki, Giza, 12622, Egypt*

† Electronic supplementary information (ESI) available. CCDC 1988241. For ESI and crystallographic data in CIF or other electronic format see DOI: 10.1039/d0ra03064c

effects. This is why urgent need of effective anti-AD agents are still compelling.[18]

The present study is focused on the construction of novel dispiro[indoline-3,2′-pyrrolidine-3′,3″-pyrrolidines] and exploring their cholinesterase properties. Rational for the targeted chemical scaffold is based on the bio-isosteric form of the indanyl nucleus of Donepezil **4** and the indolyl heterocycle of the targeted agents.[19] Additionally many natural and synthetic indole containing-compounds show promising cholinesterase inhibitory properties[20–23] including mono- and bis-spiro-indoles.[24–27] The biologically active spiro-indoles developed by our group also prompted the current study.[28–30]

Results and discussion

Chemistry

Synthetic route towards the targeted dispiro[indoline-3,2′-pyrrolidine-3′,3″-pyrrolidine]-2,2″,5″-triones **8a–l** is depicted in Scheme 1. Azomethine ylides generated from the reaction of refluxing isatins **6a–c** and sarcosine **7** in ethanol reacted regioselectively with 3-(arylmethylidene)pyrrolidine-2,5-diones **5a–e**[31–33] affording solely the corresponding dispiro analogs **8a–l** (TLC monitor). The non-stabilized azomethine ylide is formed *in situ* due to the applied reaction conditions (refluxing ethanol) through CO_2 elimination from spiro-oxazalidinone. The latter is formed *via* condensation of amino acid (sarcosine) with isatin(s).[34] The IR spectrum of compound **8a** (example of the synthesized compounds) shows strong bands at ν = 1786, 1713 cm^{-1} assignable for the stretching vibration of carbonyl groups. ^{1}H-NMR spectrum of **8a** reveals the diastereotopic methylene protons of pyrrolidinedionyl H_2C-4″ and pyrrolidinyl H_2C-5′ at δ_H = 2.37, 2.71 and 3.49, 3.84, respectively. The methine pyrrolidinyl HC-4′ is shown as a triplet signal at δ_H = 4.39. ^{13}C-NMR spectrum of **8a** reveals the pyrrolidinedionyl CH_2 (C-4″) and pyrrolidinyl CH_2 (C-5′) at δ_C = 36.7, 58.4, respectively. The spiro carbons are shown at δ_C = 61.0, 77.6 assignable for C-3′ (C-3″) and C-3 (C-2′), respectively. The methyl and methine (C-4′) carbons are revealed at δ_C = 34.6, 48.4, respectively. Additionally the carbonyl carbons are exhibited at δ_C = 173.0, 177.1 and 177.5. HSQC of compounds **8b** and **8g** support these interpretations (ESI Fig. S1–S38† show the spectral charts of the synthesized compounds). Single crystal X-ray study of compound **8c** supports the structure (Fig. 2).

X-ray studies

The ORTEP view of compound **8c** is shown in Fig. 2. The compound is in the monoclinic system and space group $P2_1/c$ with four molecules in the unit cell and one molecule in the asymmetric unit of the crystallized form. Two spiro linkages exist in **8c** attaching the central pyrrolidine ring to the pyrrolidinedione at C12 and to the indolyl heterocycle at C23. In general, the geometric parameters including both bond lengths

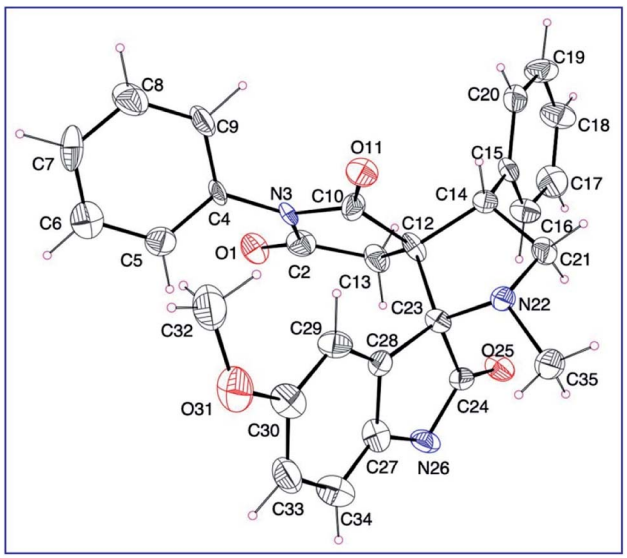

Fig. 2 An ORTEP view of **8c** showing the atom-numbering scheme. H atoms are shown as small spheres of arbitrary radii.

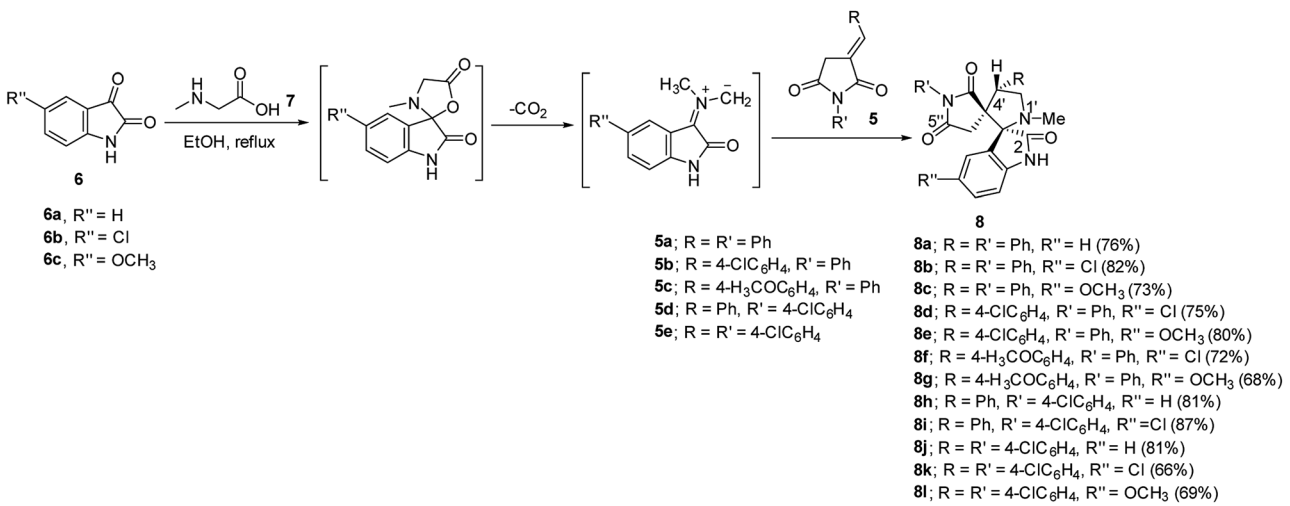

6a, R'' = H
6b, R'' = Cl
6c, R'' = OCH_3

5a; R = R' = Ph
5b; R = 4-ClC_6H_4, R' = Ph
5c; R = 4-$H_3COC_6H_4$, R' = Ph
5d; R = Ph, R' = 4-ClC_6H_4
5e; R = R' = 4-ClC_6H_4

8a; R = R' = Ph, R'' = H (76%)
8b; R = R' = Ph, R'' = Cl (82%)
8c; R = R' = Ph, R'' = OCH_3 (73%)
8d; R = 4-ClC_6H_4, R' = Ph, R'' = Cl (75%)
8e; R = 4-ClC_6H_4, R' = Ph, R'' = OCH_3 (80%)
8f; R = 4-$H_3COC_6H_4$, R' = Ph, R'' = Cl (72%)
8g; R = 4-$H_3COC_6H_4$, R' = Ph, R'' = OCH_3 (68%)
8h; R = Ph, R' = 4-ClC_6H_4, R'' = H (81%)
8i; R = Ph, R' = 4-ClC_6H_4, R'' =Cl (87%)
8j; R = R' = 4-ClC_6H_4, R'' = H (81%)
8k; R = R' = 4-ClC_6H_4, R'' = Cl (66%)
8l; R = R' = 4-ClC_6H_4, R'' = OCH_3 (69%)

Scheme 1 Synthetic route towards the targeted dispiro[indoline-3,2′-pyrrolidine-3′,3″-pyrrolidine]-2,2″,5″-triones **8a–l**.

and angles (ESI Tables S1–S3†) are in good agreement with the pre-determined structures having similar rings and moieties.[35,36]

The two phenyl rings (C4 → C9 and C15 → C20) as well as the indolyl heterocycle are planar conformations. The two pyrrolidinyl rings (C2–N3–C10–C12–C13) and (C12–C14–C21–N22–C23) are envelope conformations with the flap atoms being C12, lies 0.223 (3) Å out of the mean plane of the remaining four atoms, and N22, lies 0.662 (4) Å out of the mean plane of the remaining atoms, respectively. The sum of angles around the N22 atom is approximately 330° confirming its sp^3 hybridization. The C14 and C23 atoms occupy axial and equatorial positions with respect to the pyrrolidinedione. In the crystal, molecules are linked together by set of intermolecular C–H···O hydrogen-bonding interactions forming supramolecular assemblies (Fig. 3 and Table 1).

Biological studies

Cholinesterase inhibitory properties. AChE and BChE inhibitory properties of the synthesized dispiro-compounds **8a–l** along with Donepezil (standard reference) were presented in Table 2. From the observed experimental data it has been cleared that compounds **8e** and **8g** are superior among all the synthesized molecules with promising efficacy against both AChE and BChE (IC_{50} = 3.35, 5.63; 3.15, 4.74 μM for **8e** and **8g** against AChE and BChE, respectively). Compound **8h** also shows good cholinesterase properties (IC_{50} = 6.27, 5.34 μM against AChE and BChE, respectively). Donepezil seems more selective towards AChE rather than BChE ($SI_{(BChE/AChE)}$ = 1.31) due to its higher potency towards AChE than BChE (IC_{50} = 0.59, 0.77 μM against AChE and BChE, respectively). Similar observations are also shown by the potent synthesized agents ($SI_{(BChE/AChE)}$ = 1.68, 1.50 for compounds **8e** and **8g**, respectively). However, compound **8h** shows a different behavior (SI = 1.17, 0.85 for $SI_{(AChE/BChE)}$, $SI_{(BChE/AChE)}$, respectively).

Structure–activity relationship (SAR) based on the exhibited biological observations explain that, attachment of phenyl ring at pyrrolidinyl C-4′ seems more favorable than the *p*-chlorophenyl ring for AChE inhibitory properties (**8k** is an exception) as shown in pairs **8b**/**8d** and **8h**/**8j** (IC_{50} = 13.60, 24.30, 6.27, 20.98 μM, for **8b**, **8d**, **8h** and **8j**, respectively). Meanwhile, when *p*-methoxyphenyl ring is considered at pyrrolidinyl C-4′, better biologically active agents are optimized as shown in pairs **8b**/**8f** and **8c**/**8g** (IC_{50} = 13.60, 12.25, 102.89, 3.15 μM, for **8b**, **8f**, **8c** and **8g**, respectively). However, different SAR was noticed for BChE inhibitory properties. Where, the *p*-chlorophenyl ring containing compounds at pyrrolidinyl C-4′ are of higher BChE inhibitory properties than those of phenyl ring (compound **8h** is an exception) as shown in pairs **8b**/**8d**, **8c**/**8e** and **8i**/**8k** (IC_{50} = 42.45, 21.33, 71.75, 5.63, 35.12, 10.22 μM, for **8b**, **8d**, **8c**, **8e**, **8i** and **8k**, respectively). The same observation was also noticed for *p*-methoxyphenyl ring relative to phenyl ring due to BChE inhibitory properties similar to that of AChE as shown in pairs **8b**/**8f** and **8c**/**8g** (IC_{50} = 42.45, 20.10, 71.75 and 4.74 μM, for **8b**, **8f**, **8c** and **8g**, respectively). Molecular modeling studies can make the biological properties more understandable and identify the rules optimizing biological properties.

Table 1 Hydrogen-bond geometry (Å, °) for compound **8c**[a]

D–H···A	D–H	H···A	D···A	D–H···A
C9–H91···O1[a]	0.95(3)	2.40(5)	3.308(8)	161(2)
C21–H212···O25[a]	0.95(2)	2.56(3)	3.287(5)	133(4)

[a] Symmetry codes: −1 + *x*, *y*, *z*.

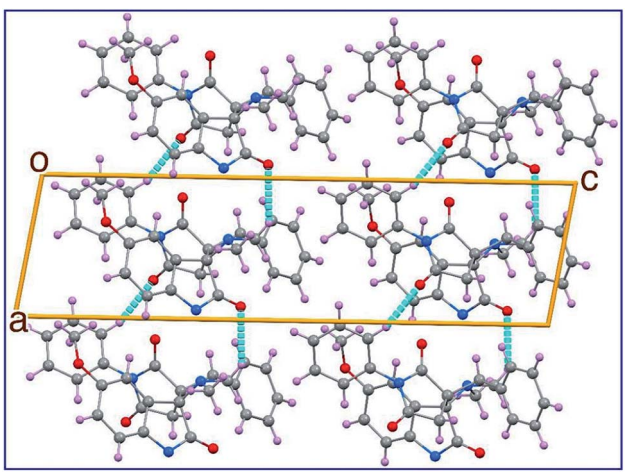

Fig. 3 Crystal packing in the unit cell of **8c** showing some hydrogen-bond interactions as dashed lines.

Antiproliferative properties. Antiproliferative properties of the synthesized agents **8a–l** were considered against RPE1 (human immortalized retinal pigment epithelial cell line) normal cell line utilizing the standard MTT (tetrazolium salt) technique.[37] The adopted technique is useful for exploring the cytotoxicity properties of the synthesized agents. From the obtained results (ESI Fig. S39†), it has been noticed that none of the synthesized agents reveal any cytotoxicological properties against the tested cell line (IC_{50} = >100.0 μM).

Acute toxicological bio-assay. The most effective agents synthesized with cholinesterase properties (**8e**, **8g** and **8h**) were subjected for acute toxicological bio-assay in mice utilizing the standard technique.[38] None of the tested agents reveal any mortality rates or toxicological symptoms (including animal body, legs, hair or tail) at the tested doses (50, 100 and 250 mg kg^{-1} mice body weight) supporting the safe utility of the tested agents at the mentioned doses.

Molecular modeling studies

Molecular modeling is an efficient technique useful for validating biological properties and identifying the parameters necessary for bio-properties beside its unique importance for developing/estimating novel hits/leads.

2D-QSAR. The cholinesterase properties observed were undertaken by CODESSA-Pro software accessible for optimizing 2D-QSAR models.[39–41] This is useful for well understanding the bio-observations and identifying the parameters necessary for bio-potency. Three descriptor QSAR models were developed due

Table 2 Cholinesterase inhibition properties of the synthesized dispiro-compounds **8a–l** and Donepezil

Entry	Compd.	IC_{50} of AChE (μM) ± SD	IC_{50} of BChE (μM) ± SD	$SI_{(AChE/BChE)}$	$SI_{(BChE/AChE)}$
1	**8a**	116.58 ± 12.28	81.75 ± 9.55	1.43	0.70
2	**8b**	13.60 ± 0.62	42.45 ± 6.26	0.32	3.12
3	**8c**	102.89 ± 10.13	71.75 ± 2.58	1.43	0.70
4	**8d**	24.30 ± 4.08	21.33 ± 2.81	1.14	0.88
5	**8e**	3.35 ± 0.03	5.63 ± 0.60	0.60	1.68
6	**8f**	12.25 ± 1.72	20.10 ± 0.16	0.61	1.64
7	**8g**	3.15 ± 0.63	4.74 ± 0.43	0.66	1.50
8	**8h**	6.27 ± 0.08	5.34 ± 0.76	1.17	0.85
9	**8i**	39.41 ± 2.23	35.12 ± 0.11	1.12	0.89
10	**8j**	20.98 ± 1.54	13.58 ± 0.37	1.54	0.65
11	**8k**	13.93 ± 0.18	10.22 ± 0.76	1.36	0.73
12	**8l**	21.97 ± 2.82	35.54 ± 0.33	0.62	1.62
13	Donepezil	0.59 ± 0.08	0.77 ± 0.01	0.77	1.31

to the AChE and BChE inhibitory properties of the synthesized dispiro-compounds **8a–l** (ESI Tables S4–S9, Fig. S40 and S41, details of the QSAR descriptors are also mentioned in the ESI).†

Goodness of the QSAR models was supported by the comparative values of the correlation coefficient (R^2) with their cross validation of leave one-out (R^2cvOO) and leave many-out (R^2cvMO) [R^2 = 0.923, 0.979; R^2cvOO = 0.882, 0.936; R^2cvMO = 0.904, 0.956, for AChE and BChE models, respectively]. Standard deviation (s^2) and Fisher criteria (F) values of the models also support their goodness (s^2 = 0.026, 0.005; F = 31.948, 122.564, for AChE and BChE models, respectively). Additionally, the correlations of the observed and predicted values "specially the high potent synthesized compounds" add good support for the attained models.

3D-pharmacophore. 3D-pharmacophore modelling of the synthesized agents **8a–l** was utilized by Discovery Studio 2.5 software (ESI Fig. S42–S45, Tables S10 and S11†). It has been noticed that, 3D-pharmacophoric modelling of the tested compounds as AChE inhibitors comprises four chemical features (two hydrophobics "H-1, H-2", one hydrogen bonding acceptor "HBA" and one positive ionisable "PosIon"). The tested compounds were fitted with variable affinity with the mentioned chemical features giving rise to different estimated properties. Aryl groups attached to C-4′ and N-1 are mapped with the hydrophobics H-1 and H-2, respectively. Meanwhile, the pyrrolidinyl carbonyl at C-2″ and pyrrolidinyl N-1′ are mapped with the HBA and PosIon, respectively. Mapping of the aryl rings at H-1 and H-2 explains their necessity in optimizing the AChE inhibitory properties. This observation supports the mentioned SAR due to the experimentally obtained results.

The 3D-pharmacophore modelling of the synthesized agents as BChE inhibitors exhibits three chemical features (hydrophobic "H", hydrogen bonding acceptor "HBA" and hydrogen bonding donor "HBD"). The aryl ring attached to the pyrrolidinyl N-1″ is mapped with the hydrophobic "H". Meanwhile, the pyrrolidinyl carbonyl at C-2″ and indolyl N-1 are mapped with the HBA and HBD, receptively. Again, mapping of the aryl ring at N-1″ supported its importance for the revealed BChE inhibitory properties.

Conclusion

In conclusion it can be stated that, the synthesized dispiro-compounds are good cholinesterase inhibitors especially compounds **8e** and **8g** which show good potency and selectivity index towards AChE over BChE similar to Donepezil (clinically used cholinesterase inhibitory drug). The attained QSAR and 3D-pharmacophore models are good enough to be considered for developing novel effective hits/leads with enhanced potency/efficacy considering the elements controlling bio-observations (mainly the aryl rings attached to the pyrrolidinedione). Additionally, the multi-component azomethine cycloaddition procedure is an accessible technique for developing the targeted dispiro[indoline-3,2′-pyrrolidine-3′,3″-pyrrolidines] in good yield (66–82%) and high regioselectivity.

Experimental

Melting points were determined on a capillary point apparatus (Stuart SMP3) equipped with a digital thermometer. IR spectra (KBr) were recorded on a Shimadzu FT-IR 8400S spectrophotometer. Reactions were monitored using thin layer chromatography (TLC) on 0.2 mm silica gel F254 plates (Merck) utilizing various solvents for elution. The chemical structures of the synthesized compounds were characterized by nuclear magnetic resonance spectra (^{1}H-NMR, ^{13}C-NMR) and determined on a Bruker NMR spectrometer (500 MHz, 125 MHz for ^{1}H and ^{13}C, respectively). ^{13}C-NMR spectra are fully decoupled. Chemical shifts were reported in parts per million (ppm) using the deuterated solvent peak or tetramethylsilane as an internal standard. Colorimetric enzyme inhibitory assays were performed in 96-well plates and the absorbance was recorded utilizing a microplate reader (Infinite F50, Tecan, Switzerland).

Synthesis of dispiro[indoline-3,2′-pyrrolidine-3′,3″-pyrrolidines] 8a–l (general procedure)

A mixture of equimolar amount of the appropriate **5a–e** (5 mmol), isatin **6a–c** and sarcosine **7** in absolute ethanol (25 mL) was boiled under reflux for the specific time. The separated solid while boiling, was collected and crystallized from

a suitable solvent affording the corresponding **8a–g,i–k**. In case of **8h,l** the clear reaction mixture was stored at room temperature (20–25 °C) overnight. So, the separated solid was collected and purified by crystallization from a suitable solvent.

1′-Methyl-1″,4′-diphenyldispiro[indoline-3,2′-pyrrolidine-3′,3″-pyrrolidine]-2,2″,5″-trione (8a)

It was obtained from the reaction of **5a** with **6a** and sarcosine for 10 h as colorless microcrystals from *n*-butanol with mp 236–238 °C and yield 76% (1.65 g). IR: ν_{max}/cm^{-1} 3480, 3067, 2870, 1786, 1713, 1616, 1597. ^{1}H-NMR (DMSO-d_6) δ (ppm): 2.10 (s, 3H, NCH_3), 2.37 (d, J = 18.3 Hz, 1H, upfield H of pyrrolidinedionyl H_2C-4″), 2.71 (d, J = 18.3 Hz, 1H, downfield H of pyrrolidinedionyl H_2C-4″), 3.49 (t, J = 8.6 Hz, 1H, upfield H of pyrrolidinyl H_2C-5′), 3.84 (t, J = 9.3 Hz, 1H, downfield H of pyrrolidinyl H_2C-5′), 4.39 (t, J = 8.9 Hz, 1H, pyrrolidinyl HC-4′), 6.75 (dd, J = 1.8, 7.7 Hz, 2H, arom. H), 6.89 (d, J = 7.7 Hz, 1H, arom. H), 6.99 (t, J = 7.6 Hz, 1H, arom. H), 7.21 (d, J = 7.4 Hz, 1H, arom. H), 7.30–7.43 (m, 7H, arom. H), 7.49 (d, J = 7.4 Hz, 2H, arom. H), 10.78 (s, 1H, NH). ^{13}C-NMR (DMSO-d_6) δ (ppm): 34.6 (NCH_3), 36.7 [pyrrolidinedionyl CH_2 (C-4″)], 48.4 [pyrrolidinyl CH (C-4′)], 58.4 [pyrrolidinyl CH_2 (C-5′)], 61.0 [C-3′ (C-3″)], 77.6 [C-3 (C-2′)], 110.0, 122.0, 125.0, 126.5, 126.8, 127.4, 128.4, 128.6, 128.7, 129.9, 131.6, 137.9, 142.7 (arom. C), 173.0, 177.1, 177.5 (CO). Anal. calcd for $C_{27}H_{23}N_3O_3$ (437.50): C, 74.13; H, 5.30; N, 9.60. Found: C, 74.24; H, 5.49; N, 9.68.

5-Chloro-1′-methyl-1″,4′-diphenyldispiro[indoline-3,2′-pyrrolidine-3′,3″-pyrrolidine]-2,2″,5″-trione (8b)

It was obtained from the reaction of **5a** with **6b** and sarcosine for 12 h as colorless microcrystals from *N*,*N*-dimethylformamide–water (2–1 v/v) with mp 253–255 °C and yield 82% (1.94 g). IR: ν_{max}/cm^{-1} 3472, 3063, 2874, 1782, 1713, 1616, 1597. ^{1}H-NMR (DMSO-d_6) δ (ppm): 2.11 (s, 3H, NCH_3), 2.39 (d, J = 18.2 Hz, 1H, upfield H of pyrrolidinedionyl H_2C-4″), 2.70 (d, J = 18.2 Hz, 1H, downfield H of pyrrolidinedionyl H_2C-4″), 3.51 (t, J = 8.6 Hz, 1H, upfield H of pyrrolidinyl H_2C-5′), 3.80 (t, J = 9.3 Hz, 1H, downfield H of pyrrolidinyl H_2C-5′), 4.37 (t, J = 9.0 Hz, 1H, pyrrolidinyl HC-4′), 6.82 (dd, J = 1.6, 8.0 Hz, 2H, arom. H), 6.91 (d, J = 8.3 Hz, 1H, arom. H), 7.19 (d, J = 2.2 Hz, 1H, arom. H), 7.33 (t, J = 7.3 Hz, 1H, arom. H), 7.37–7.43 (m, 6H, arom. H), 7.48 (d, J = 7.4 Hz, 2H, arom. H), 10.94 (s, 1H, NH). ^{13}C-NMR (DMSO-d_6) δ (ppm): 34.6 (NCH_3), 36.5 [pyrrolidinedionyl CH_2 (C-4″)], 48.5 [pyrrolidinyl CH (C-4′)], 58.3 [pyrrolidinyl CH_2 (C-5′)], 61.0 [C-3′ (C-3″)], 77.5 [C-3 (C-2′)], 111.5, 126.2, 126.3, 126.6, 127.0, 127.4, 128.5, 128.6, 128.7, 129.9, 130.0, 131.5, 137.6, 141.7 (arom. C), 172.8, 176.7, 177.4 (CO). Anal. calcd for $C_{27}H_{22}ClN_3O_3$ (471.94): C, 68.72; H, 4.70; N, 8.90. Found: C, 68.96; H, 4.84; N, 9.06.

5-Methoxy-1′-methyl-1″,4′-diphenyldispiro[indoline-3,2′-pyrrolidine-3′,3″-pyrrolidine]-2,2″,5″-trione (8c)

It was obtained from the reaction of **5a** with **6c** and sarcosine for 12 h as colorless microcrystals from *n*-butanol with mp 253–255 °C and yield 73% (1.70 g). IR: ν_{max}/cm^{-1} 3472, 3063, 2870, 1778, 1713, 1697, 1605, 1497. ^{1}H-NMR (DMSO-d_6) δ (ppm): 2.11 (s, 3H, NCH_3), 2.36 (d, J = 18.2 Hz, 1H, upfield H of pyrrolidinedionyl H_2C-4″), 2.64 (d, J = 18.2 Hz, 1H, downfield H of pyrrolidinedionyl H_2C-4″), 3.49 (t, J = 8.5 Hz, 1H, upfield H of pyrrolidinyl H_2C-5′), 3.55 (s, 3H, OCH_3), 3.83 (t, J = 9.3 Hz, 1H, downfield H of pyrrolidinyl H_2C-5′), 4.37 (t, J = 8.9 Hz, 1H, pyrrolidinyl HC-4′), 6.73–6.75 (m, 3H, arom. H), 6.82 (d, J = 8.4 Hz, 1H, arom. H), 6.90 (dd, J = 2.6, 8.5 Hz, 1H, arom. H), 7.31–7.42 (m, 6H, arom. H), 7.51 (d, J = 7.4 Hz, 2H, arom. H), 10.63 (s, 1H, NH). ^{13}C-NMR (DMSO-d_6) δ (ppm): 34.6 (NCH_3), 36.8 [pyrrolidinedionyl CH_2 (C-4″)], 48.1 [pyrrolidinyl CH (C-4′)], 55.1 (OCH_3), 58.7 [pyrrolidinyl CH_2 (C-5′)], 61.4 [C-3′ (C-3″)], 77.9 [C-3 (C-2′)], 110.4, 113.2, 114.6, 126.2, 126.7, 127.3, 128.4, 128.57, 128.61, 130.1, 131.6, 135.8, 138.1, 154.9 (arom. C), 172.9, 177.0, 177.6 (CO). Anal. calcd for $C_{28}H_{25}N_3O_4$ (467.53): C, 71.93; H, 5.39; N, 8.99. Found: C, 71.99; H, 5.60; N, 9.22.

5-Chloro-4′-(4-chlorophenyl)-1′-methyl-1″-phenyldispiro[indoline-3,2′-pyrrolidine-3′,3″-pyrrolidine]-2,2″,5″-trione (8d)

It was obtained from the reaction of **5b** with **6b** and sarcosine for 12 h as colorless microcrystals from *n*-butanol with mp 232–234 °C and yield 75% (1.89 g). IR: ν_{max}/cm^{-1} 3487, 3059, 2874, 1790, 1713, 1620, 1597. ^{1}H-NMR (DMSO-d_6) δ (ppm): 2.11 (s, 3H, NCH_3), 2.42 (d, J = 18.1 Hz, 1H, upfield H of pyrrolidinedionyl H_2C-4″), 2.67 (d, J = 18.2 Hz, 1H, downfield H of pyrrolidinedionyl H_2C-4″), 3.52 (t, J = 8.7 Hz, 1H, upfield H of pyrrolidinyl H_2C-5′), 3.74 (t, J = 9.3 Hz, 1H, downfield H of pyrrolidinyl H_2C-5′), 4.37 (t, J = 8.9 Hz, 1H, pyrrolidinyl HC-4′), 6.83 (dd, J = 1.5, 8.0 Hz, 2H, arom. H), 6.92 (d, J = 8.3 Hz, 1H, arom. H), 7.16 (d, J = 2.2 Hz, 1H, arom. H), 7.38–7.41 (m, 4H, arom. H), 7.47 (d, J = 8.5 Hz, 2H, arom. H), 7.53 (d, J = 8.5 Hz, 2H, arom. H), 10.97 (s, 1H, NH). ^{13}C-NMR (DMSO-d_6) δ (ppm): 34.6 (NCH_3), 36.6 [pyrrolidinedionyl CH_2 (C-4″)], 47.7 [pyrrolidinyl CH (C-4′)], 58.7 [pyrrolidinyl CH_2 (C-5′)], 61.0 [C-3′ (C-3″)], 77.6 [C-3 (C-2′)], 111.6, 126.2, 126.3, 126.6, 126.9, 128.46, 128.54, 128.7, 130.0, 131.5, 132.0, 132.1, 136.8, 141.7 (arom. C), 172.8, 176.8, 177.3 (CO). Anal. calcd for $C_{27}H_{21}Cl_2N_3O_3$ (506.38): C, 64.04; H, 4.18; N, 8.30. Found: C, 63.74; H, 4.35; N, 8.44.

4′-(4-Chlorophenyl)-5-methoxy-1′-methyl-1″-phenyldispiro[indoline-3,2′-pyrrolidine-3′,3″-pyrrolidine]-2,2″,5″-trione (8e)

It was obtained from the reaction of **5b** with **6c** and sarcosine for 14 h as colorless microcrystals from *n*-butanol with mp 228–230 °C and yield 80% (2.00 g). IR: ν_{max}/cm^{-1} 3487, 3059, 2874, 1786, 1713, 1601, 1489. ^{1}H-NMR (DMSO-d_6) δ (ppm): 2.11 (s, 3H, NCH_3), 2.39 (d, J = 18.1 Hz, 1H, upfield H of pyrrolidinedionyl H_2C-4″), 2.62 (d, J = 18.1 Hz, 1H, downfield H of pyrrolidinedionyl H_2C-4″), 3.51 (t, J = 8.6 Hz, 1H, upfield H of pyrrolidinyl H_2C-5′), 3.54 (s, 3H, OCH_3), 3.77 (t, J = 9.2 Hz, 1H, downfield H of pyrrolidinyl H_2C-5′), 4.37 (t, J = 8.9 Hz, 1H, pyrrolidinyl HC-4′), 6.70 (d, J = 2.5 Hz, 1H, arom. H), 6.75 (dd, J = 2.0, 7.4 Hz, 2H, arom. H), 6.83 (d, J = 8.4 Hz, 1H, arom. H), 6.90 (dd, J = 2.6, 8.5 Hz, 1H, arom. H), 7.36–7.38 (m, 3H, arom. H), 7.47 (d, J = 8.5 Hz, 2H, arom. H), 7.55 (d, J = 8.4 Hz, 2H, arom. H), 10.66 (s, 1H, NH). ^{13}C-NMR (DMSO-d_6) δ (ppm): 34.5 (NCH_3), 36.9 [pyrrolidinedionyl CH_2 (C-4″)], 47.3 [pyrrolidinyl CH (C-4′)], 55.1 (OCH_3), 59.0 [pyrrolidinyl CH_2 (C-5′)], 61.3 [C-3′ (C-3″)], 77.9 [C-3

(C-2′)], 110.5, 113.0, 114.6, 126.1, 126.7, 128.4, 128.5, 128.53, 131.6, 132.0, 132.1, 135.8, 137.3, 155.0 (arom. C), 172.9, 177.1, 177.4 (CO). Anal. calcd for $C_{28}H_{24}ClN_3O_4$ (501.97): C, 67.00; H, 4.82; N, 8.37. Found: C, 67.19; H, 5.04; N, 8.42.

5-Chloro-4′-(4-methoxyphenyl)-1′-methyl-1″-phenyldispiro[indoline-3,2′-pyrrolidine-3′,3″-pyrrolidine]-2,2″,5″-trione (8f)

It was obtained from the reaction of **5c** with **6b** and sarcosine for 12 h as colorless microcrystals from *n*-butanol with mp 223–225 °C and yield 72% (1.80 g). IR: ν_{max}/cm^{-1} 3483, 3078, 2832, 1786, 1713, 1616. ^{1}H-NMR (DMSO-d_6) δ (ppm): 2.11 (s, 3H, NCH_3), 2.42 (d, J = 18.2 Hz, 1H, upfield H of pyrrolidinedionyl H_2C-4″), 2.68 (d, J = 18.2 Hz, 1H, downfield H of pyrrolidinedionyl H_2C-4″), 3.48 (t, J = 8.6 Hz, 1H, upfield H of pyrrolidinyl H_2C-5′), 3.76 (s, 3H, OCH_3), 3.76 (t, J = 9.3 Hz, 1H, downfield H of pyrrolidinyl H_2C-5′), 4.32 (t, J = 9.0 Hz, 1H, pyrrolidinyl HC-4′), 6.84 (dd, J = 1.4, 8.0 Hz, 2H, arom. H), 6.91 (d, J = 8.3 Hz, 1H, arom. H), 6.97 (d, J = 8.7 Hz, 2H, arom. H), 7.21 (d, J = 2.1 Hz, 1H, arom. H), 7.37–7.42 (m, 6H, arom. H), 10.92 (s, 1H, NH). ^{13}C-NMR (DMSO-d_6) δ (ppm): 34.6 (NCH_3), 36.4 [pyrrolidinedionyl CH_2 (C-4″)], 48.0 [pyrrolidinyl CH (C-4′)], 55.0 (OCH_3), 58.4 [pyrrolidinyl CH_2 (C-5′)], 61.0 [C-3′ (C-3″)], 77.5 [C-3 (C-2′)], 111.5, 114.0, 126.2, 126.4, 126.6, 127.1, 128.5, 128.8, 129.3, 129.8, 131.0, 131.5, 141.7, 158.5 (arom. C), 172.9, 176.7, 177.6 (CO). Anal. calcd for $C_{28}H_{24}ClN_3O_4$ (501.97): C, 67.00; H, 4.82; N, 8.37. Found: C, 67.20; H, 4.66; N, 8.18.

5-Methoxy-4′-(4-methoxyphenyl)-1′-methyl-1″-phenyldispiro[indoline-3,2′-pyrrolidine-3′,3″-pyrrolidine]-2,2″,5″-trione (8g)

It was obtained from the reaction of **5c** with **6c** and sarcosine for 15 h as colorless microcrystals from *n*-butanol with mp 217–219 °C and yield 68% (1.68 g). IR: ν_{max}/cm^{-1} 3480, 3075, 2959, 1782, 1713, 1601. ^{1}H-NMR (DMSO-d_6) δ (ppm): 2.11 (s, 3H, NCH_3), 2.38 (d, J = 18.3 Hz, 1H, upfield H of pyrrolidinedionyl H_2C-4″), 2.62 (d, J = 18.2 Hz, 1H, downfield H of pyrrolidinedionyl H_2C-4″), 3.46 (t, J = 8.5 Hz, 1H, upfield H of pyrrolidinyl H_2C-5′), 3.55 (s, 3H, OCH_3), 3.76 (s, 3H, OCH_3), 3.79 (t, J = 9.2 Hz, 1H, downfield H of pyrrolidinyl H_2C-5′), 4.32 (t, J = 8.9 Hz, 1H, pyrrolidinyl HC-4′), 6.74–6.76 (m, 3H, arom. H), 6.81 (d, J = 8.4 Hz, 1H, arom. H), 6.89 (dd, J = 2.6, 8.5 Hz, 1H, arom. H), 6.97 (d, J = 8.8 Hz, 2H, arom. H), 7.37–7.43 (m, 5H, arom. H), 10.61 (s, 1H, NH). ^{13}C-NMR (DMSO-d_6) δ (ppm): 34.6 (NCH_3), 36.7 [pyrrolidinedionyl CH_2 (C-4″)], 47.6 [pyrrolidinyl CH (C-4′)], 55.0 (OCH_3), 55.1 (OCH_3), 58.8 [pyrrolidinyl CH_2 (C-5′)], 61.4 [C-3′ (C-3″)], 77.9 [C-3 (C-2′)], 110.4, 113.2, 114.0, 114.5, 126.3, 126.7, 128.4, 128.6, 129.8, 131.1, 131.6, 135.8, 154.9, 158.4 (arom. C), 173.0, 177.1, 177.7 (CO). Anal. calcd for $C_{29}H_{27}N_3O_5$ (497.55): C, 70.01; H, 5.47; N, 8.45. Found: C, 69.87; H, 5.40; N, 8.25.

1″-(4-Chlorophenyl)-1′-methyl-4′-phenyldispiro[indoline-3,2′-pyrrolidine-3′,3″-pyrrolidine]-2,2″,5″-trione (8h)

It was obtained from the reaction of **5d** with **6a** and sarcosine for 10 h as pale yellow microcrystals from *n*-butanol with mp 208–210 °C (lit. 189–190 °C (ref. 33)) and yield 81% (1.90 g). IR: ν_{max}/cm^{-1} 3480, 3067, 2951, 1778, 1713, 1616, 1597. ^{1}H-NMR (DMSO-d_6) δ (ppm): 2.09 (s, 3H, NCH_3), 2.39 (d, J = 18.2 Hz, 1H, upfield H of pyrrolidinedionyl H_2C-4″), 2.67 (d, J = 18.2 Hz, 1H, downfield H of pyrrolidinedionyl H_2C-4″), 3.49 (t, J = 8.6 Hz, 1H, upfield H of pyrrolidinyl H_2C-5′), 3.82 (t, J = 9.3 Hz, 1H, downfield H of pyrrolidinyl H_2C-5′), 4.37 (t, J = 8.9 Hz, 1H, pyrrolidinyl HC-4′), 6.79 (dd, J = 2.0, 6.8 Hz, 2H, arom. H), 6.88 (d, J = 7.7 Hz, 1H, arom. H), 6.97 (t, J = 7.6 Hz, 1H, arom. H), 7.16 (d, J = 7.4 Hz, 1H, arom. H), 7.28–7.33 (m, 2H, arom. H), 7.39–7.50 (m, 6H, arom. H), 10.78 (s, 1H, NH). ^{13}C-NMR (DMSO-d_6) δ (ppm): 34.5 (NCH_3), 36.9 [pyrrolidinedionyl CH_2 (C-4″)], 48.2 [pyrrolidinyl CH (C-4′)], 58.6 [pyrrolidinyl CH_2 (C-5′)], 61.2 [C-3′ (C-3″)], 77.6 [C-3 (C-2′)], 110.0, 122.0, 125.0, 126.2, 127.3, 128.5, 128.6, 128.7, 129.99, 130.0, 130.3, 132.9, 138.0, 142.7 (arom. C), 172.7, 177.1, 177.3 (CO). Anal. calcd for $C_{27}H_{22}ClN_3O_3$ (471.94): C, 68.72; H, 4.70; N, 8.90. Found: C, 68.95; H, 4.86; N, 8.81.

5-Chloro-1″-(4-chlorophenyl)-1′-methyl-4′-phenyldispiro[indoline-3,2′-pyrrolidine-3′,3″-pyrrolidine]-2,2″,5″-trione (8i)

It was obtained from the reaction of **5d** with **6b** and sarcosine for 10 h as colorless microcrystals from *n*-butanol with mp 240–242 °C and yield 87% (2.20 g). IR: ν_{max}/cm^{-1} 3476, 3102, 2839, 1778, 1713, 1620. ^{1}H-NMR (DMSO-d_6) δ (ppm): 2.12 (s, 3H, NCH_3), 2.42 (d, J = 18.2 Hz, 1H, upfield H of pyrrolidinedionyl H_2C-4″), 2.70 (d, J = 18.2 Hz, 1H, downfield H of pyrrolidinedionyl H_2C-4″), 3.51 (t, J = 8.6 Hz, 1H, upfield H of pyrrolidinyl H_2C-5′), 3.81 (t, J = 9.3 Hz, 1H, downfield H of pyrrolidinyl H_2C-5′), 4.37 (t, J = 8.9 Hz, 1H, pyrrolidinyl HC-4′), 6.88 (d, J = 8.7 Hz, 2H, arom. H), 6.92 (d, J = 8.3 Hz, 1H, arom. H), 7.17 (d, J = 2.2 Hz, 1H, arom. H), 7.31–7.42 (m, 4H, arom. H), 7.48–7.50 (m, 4H, arom. H), 10.95 (s, 1H, NH). ^{13}C-NMR (DMSO-d_6) δ (ppm): 34.6 (NCH_3), 36.6 [pyrrolidinedionyl CH_2 (C-4″)], 48.5 [pyrrolidinyl CH (C-4′)], 58.5 [pyrrolidinyl CH_2 (C-5′)], 61.1 [C-3′ (C-3″)], 77.5 [C-3 (C-2′)], 111.6, 126.22, 126.24, 127.0, 127.4, 128.3, 128.6, 128.8, 129.9, 130.1, 130.3, 133.0, 137.6, 141.7 (arom. C), 172.6, 176.7, 177.2 (CO). Anal. calcd for $C_{27}H_{21}Cl_2N_3O_3$ (506.38): C, 64.04; H, 4.18; N, 8.30. Found: C, 64.21; H, 4.26; N, 8.41.

1″,4′-Bis(4-chlorophenyl)-1′-methyldispiro[indoline-3,2′-pyrrolidine-3′,3″-pyrrolidine]-2,2″,5″-trione (8j)

It was obtained from the reaction of **5e** with **6a** and sarcosine for 10 h as colorless microcrystals from *n*-butanol with mp 225–227 °C (lit. 224–226 °C (ref. 33)) and yield 81% (2.05 g). IR: ν_{max}/cm^{-1} 3487, 3063, 2878, 1790, 1717, 1620, 1597, 1493. ^{1}H-NMR (DMSO-d_6) δ (ppm): 2.08 (s, 3H, NCH_3), 2.41 (d, J = 18.1 Hz, 1H, upfield H of pyrrolidinedionyl H_2C-4″), 2.64 (d, J = 18.1 Hz, 1H, downfield H of pyrrolidinedionyl H_2C-4″), 3.51 (t, J = 8.6 Hz, 1H, upfield H of pyrrolidinyl H_2C-5′), 3.75 (t, J = 9.2 Hz, 1H, downfield H of pyrrolidinyl H_2C-5′), 4.36 (t, J = 8.9 Hz, 1H, pyrrolidinyl HC-4′), 6.79 (dd, J = 1.9, 6.8 Hz, 2H, arom. H), 6.89 (d, J = 7.7 Hz, 1H, arom. H), 6.97 (t, J = 7.7 Hz, 1H, arom. H), 7.13 (d, J = 7.4 Hz, 1H, arom. H), 7.30 (dt, J = 1.0, 7.7 Hz, 1H, arom. H), 7.44–7.47 (m, 4H, arom. H), 7.53 (d, J = 8.5 Hz, 2H, arom. H), 10.80 (s, 1H, NH). ^{13}C-NMR (DMSO-d_6) δ (ppm): 34.5 (NCH_3), 36.9 [pyrrolidinedionyl CH_2 (C-4″)], 47.4 [pyrrolidinyl CH (C-4′)], 58.9 [pyrrolidinyl CH_2 (C-5′)], 61.1 [C-3′ (C-3″)], 77.6

[C-3 (C-2′)], 110.1, 122.1, 124.8, 126.1, 128.5, 128.7, 130.1, 130.3, 132.0, 132.1, 132.9, 137.2, 142.7 (arom. C), 172.7, 177.2 (CO). Anal. calcd for $C_{27}H_{21}Cl_2N_3O_3$ (506.38): C, 64.04; H, 4.18; N, 8.30. Found: C, 63.88; H, 3.97; N, 8.06.

5-Chloro-1″,4′-bis(4-chlorophenyl)-1′-methyldispiro[indoline-3,2′-pyrrolidine-3′,3″-pyrrolidine]-2,2″,5″-trione (8k)

It was obtained from the reaction of **5e** with **6b** and sarcosine for 9 h as colorless microcrystals from *n*-butanol with mp 236–238 °C and yield 66% (1.77 g). IR: ν_{max}/cm^{-1} 3487, 3105, 2874, 1786, 1713, 1620, 1493. ^{1}H-NMR (DMSO-d_6) δ (ppm): 2.10 (s, 3H, NCH_3), 2.42 (d, J = 18.1 Hz, 1H, upfield H of pyrrolidinedionyl H_2C-4″), 2.65 (d, J = 18.0 Hz, 1H, downfield H of pyrrolidinedionyl H_2C-4″), 3.52 (t, J = 8.7 Hz, 1H, upfield H of pyrrolidinyl H_2C-5′), 3.72 (t, J = 9.3 Hz, 1H, downfield H of pyrrolidinyl H_2C-5′), 4.35 (t, J = 8.9 Hz, 1H, pyrrolidinyl HC-4′), 6.87 (dd, J = 2.0, 6.8 Hz, 2H, arom. H), 6.91 (d, J = 8.3 Hz, 1H, arom. H), 7.11 (d, J = 2.2 Hz, 1H, arom. H), 7.37 (dd, J = 2.2, 8.3 Hz, 1H, arom. H), 7.47–7.54 (m, 6H, arom. H), 10.97 (s, 1H, NH). ^{13}C-NMR (DMSO-d_6) δ (ppm): 34.6 (NCH_3), 36.7 [pyrrolidinedionyl CH_2 (C-4″)], 47.5 [pyrrolidinyl CH (C-4′)], 58.8 [pyrrolidinyl CH_2 (C-5′)], 61.1 [C-3′ (C-3″)], 77.5 [C-3 (C-2′)], 111.6, 126.0, 126.3, 126.9, 128.2, 128.5, 128.8, 130.0, 130.3, 132.06, 132.1, 132.9, 136.8, 141.7 (arom. C), 172.5, 176.7, 177.1 (CO). Anal. calcd for $C_{27}H_{20}Cl_3N_3O_3$ (540.83): C, 59.96; H, 3.73; N, 7.77. Found: C, 60.10; H, 3.84; N, 7.64.

1″,4′-Bis(4-chlorophenyl)-5-methoxy-1′-methyldispiro[indoline-3,2′-pyrrolidine-3′,3″-pyrrolidine]-2,2″,5″-trione (8l)

It was obtained from the reaction of **5e** with **6c** and sarcosine for 12 h as colorless microcrystals from *n*-butanol with mp 247–249 °C and yield 69% (1.84 g). IR: ν_{max}/cm^{-1} 3476, 3210, 2870, 1778, 1697, 1632, 1605. ^{1}H-NMR (DMSO-d_6) δ (ppm): 2.11 (s, 3H, NCH_3), 2.41 (d, J = 18.0 Hz, 1H, upfield H of pyrrolidinedionyl H_2C-4″), 2.62 (d, J = 18.0 Hz, 1H, downfield H of pyrrolidinedionyl H_2C-4″), 3.51 (t, J = 8.6 Hz, 1H, upfield H of pyrrolidinyl H_2C-5′), 3.55 (s, 3H, OCH_3), 3.77 (t, J = 9.2 Hz, 1H, downfield H of pyrrolidinyl H_2C-5′), 4.38 (t, J = 8.9 Hz, 1H, pyrrolidinyl HC-4′), 6.68 (d, J = 2.5 Hz, 1H, arom. H), 6.78–6.91 (m, 4H, arom. H), 7.45–7.48 (m, 3H, arom. H), 7.56 (d, J = 8.5 Hz, 2H, arom. H), 10.67 (s, 1H, NH). ^{13}C-NMR (DMSO-d_6) δ (ppm): 34.5 (NCH_3), 37.0 [pyrrolidinedionyl CH_2 (C-4″)], 47.2 [pyrrolidinyl CH (C-4′)], 55.1 (OCH_3), 59.2 [pyrrolidinyl CH_2 (C-5′)], 61.5 [C-3' (C-3″)], 77.9 [C-3 (C-2′)], 110.5, 112.9, 114.6, 126.1, 128.4, 128.5, 128.6, 130.4, 132.0, 132.2, 132.9, 135.7, 137.3, 155.0 (arom. C), 172.7, 177.1 (CO). Anal. calcd for $C_{28}H_{23}Cl_2N_3O_4$ (536.41): C, 62.70; H, 4.32; N, 7.83. Found: C, 62.91; H, 4.14; N, 8.00.

X-ray studies

The experimental procedure was mentioned in the ESI.†

Biological studies

All the biological procedures utilized obey the standards and approved by the Research Ethics Committee, National Research Centre, Egypt (associated with project ID: 12060101). All the experiments were performed following the relevant guidelines and regulations.

Chloinesterase inhibitory activity studies. The assays were undertaken by the standard technique.[42] Briefly, 170 μL of Tris–HCl buffer (200 mM, pH 7.5) was added followed by 20 μL at different concentrations of tested compounds (125–0.977 μg mL^{-1}) and then 20 μL of the enzyme solution (0.1 U mL^{-1}). After incubation period of 10 min at 25 °C, 40 μL of DTNB (dithio-bis-(2-nitrobenzoic acid)) and then 20 μL of the substrate (1.11 mM) were added. Butyrylthiocholine iodide and acetylthiocholine were utilized as substrates in BChE and AChE assays, respectively, where DTNB was served as indicator. All compounds were dissolved in MeOH. The intensity of the developed color was measured at 405 nm using a microplate reader (reading A) and control without the inhibitor were measured (reading B). Blank assays were performed by replacing the enzyme (20 μL) with buffer and their absorbances were recorded for correction of the spontaneous lysis of the indicator or inherent color of the inhibitor. Linear regression was performed for calculation of the IC_{50} (50% inhibitory concentration). Microsoft EXCEL 2010 program and graph pad instate 6.0 software were used for the data analysis.

$$\% \text{ Inhibition} = [1 - (\text{corrected A}/\text{corrected B})] \times 100$$

Selectivity index (SI) for acetyl and butyryl cholinesterases was calculated as follow:

$$SI_{(AChE/BChE)} = IC_{50}\ (AChE)/IC_{50}\ (BChE)$$

$$SI_{(BChE/AChE)} = IC_{50}\ (AChE)/IC_{50}\ (BChE)$$

Antiproliferative properties. The synthesized agents **8a–l** were screened against RPE1 (human immortalized retinal pigment epithelial cell line) normal cell line to investigate their cytotoxicity by the standard mitochondrial dependent reduction of yellow MTT [3-(4,5-dimethylthiazol-2-yl)-2,5-diphenyltetrazolium bromide] to purple formazan technique.[37] Cells were suspended in DMEM in addition to 1% antibiotic–antimycotic mixture (10 000 μg mL^{-1} potassium penicillin, 10 000 μg mL^{-1} streptomycin sulfate and 25 μg mL^{-1} amphotericin B), 10% fetal bovine serum and 1% L-glutamine at 37 °C, under 5% CO_2 and 95% humidity. Cells were seeded at concentration of 30 000 cells per well in fresh complete growth medium in 96-well tissue culture microtiter plates for 24 h. Media was aspirated, fresh complete medium was added and cells were incubated with different concentrations of the tested compound to give a final concentration of (100, 50, 25 and 12.5 μM). 0.5% DMSO was used as negative control. Triplicate wells were prepared for each individual dose. After 72 h of incubation, medium was aspirated, 40 μl MTT salt (2.5 mg mL^{-1}) were added to each well and incubated for further 4 h at 37 °C. To stop the reaction and dissolve the formed crystals, 150 μL of 10% sodium dodecyl sulfate (SDS) in deionized water were added to each well and incubated overnight at 37 °C. The

absorbance was then measured at 570 nm and a reference wavelength of 595 nm.

Data were collected as mean values for experiments performed in triplicates for each individual dose which had been measured by MTT assay. Control experiments did not exhibit significant change compared to the DMSO vehicle. The percentage of cell survival was calculated according to the following equation.

$$\text{Surviving fraction} = \frac{\text{Optical density(O.D.)of treated cells}}{\text{O.D. of control cells}}$$

The IC_{50} (concentration required to produce 50% inhibition of cell growth compared to the control experiment) can was determined using Graph-Pad PRISM version-5 software. Statistical calculations for determination of the mean and standard error values were determined by SPSS 16 software. The observed anti-proliferative properties are presented ESI Fig. S39.†

Acute toxicological bio-assay. The most effective agents synthesized with cholinesterase properties (**8e**, **8g** and **8h**) were subjected for acute toxicological bio-assay in mice utilizing the standard technique.[38] Albino mice weighing 20–25 g were divided into 4 groups of 6 mice each. Administrations of the tested compounds dissolved in saline solution (0.9%) by the aid of few drops of Tween 80 were given intraperitoneally in 50, 100 and 250 mg kg^{-1} (mice body weight). The control group was given a saline solution only with few drops of Tween 80. The toxic symptoms and mortality rates were recorded 24 h post-administration in each group.

Molecular modeling studies

The experimental procedures in details were mentioned in the ESI.†

Conflicts of interest

There is no conflict to declare.

Acknowledgements

This work was supported financially by National Research Centre, Egypt, project ID: 12060101.

Notes and references

1 https://www.who.int/news-room/fact-sheets/detail/dementia.
2 R. Malek, R. L. Arribas, A. Palomino-Antolin, P. Totoson, C. Demougeot, T. Kobrlova, O. Soukup, I. Iriepa, I. Moraleda, D. Diez-Iriepa, J. Godyń, D. Panek, B. Malawska, M. Głuch-Lutwin, B. Mordyl, A. Siwek, F. Chabchoub, J. Marco-Contelles, K. Kiec-Kononowicz, J. Egea, C. de los Rios and L. Ismaili, New dual small molecules for Alzheimer's disease therapy combining histamine H_3 receptor (H3R) antagonism and calcium channels blockade with additional cholinesterase inhibition, *J. Med. Chem.*, 2019, **62**, 11416–11422.
3 S. Rizzo, C. Rivière, L. Piazzi, A. Bisi, S. Gobbi, M. Bartolini, V. Andrisano, F. Morroni, A. Tarozzi, J.-P. Monti and A. Rampa, Benzofuran-based hybrid compounds for the inhibition of cholinesterase activity, β amyloid aggregation, and Aβ neurotoxicity, *J. Med. Chem.*, 2008, **51**, 2883–2886.
4 A. Morsy and P. C. Trippier, Current and emerging pharmacological targets for the treatment of Alzheimer's disease, *J. Alzheimer's Dis.*, 2019, **72**, S145–S176.
5 X. Li, H. Wang, Z. Lu, X. Zheng, W. Ni, J. Zhu, Y. Fu, F. Lian, N. Zhang, J. Li, H. Zhang and F. Mao, Development of multifunctional primidinylthiourea derivatives as potential anti-Alzheimer agents, *J. Med. Chem.*, 2016, **59**, 8326–8344.
6 P. W. Elsinghorst, C. M. G. Tanarro and M. Gütschow, Novel heterobivalent Tacrine derivatives as cholinesterase inhibitors with notable selectivity toward butyrylcholinesterase, *J. Med. Chem.*, 2006, **49**, 7540–7544.
7 M. L. Crismon, Tacrine: first drug approved for Alzheimer's disease, *Ann. Pharmacother.*, 1994, **28**, 744–751.
8 https://www.drugbank.ca/drugs/DB00382.
9 S. Hamulakova, L. Janovec, M. Hrabinova, K. Spilovska, J. Korabecny, P. Kristian, K. Kuca and J. Imrich, Synthesis and biological evaluation of novel Tacrine derivatives and Tacrine-coumarin hybrids as cholinesterase inhibitors, *J. Med. Chem.*, 2014, **57**, 7073–7084.
10 L. Fang, D. Appenroth, M. Decker, M. Kiehntopf, C. Roegler, T. Deufel, C. Fleck, S. Peng, Y. Zhang and J. Lehmann, Synthesis and biological evaluation of NO-donor-Tacrine hybrids as hepatoprotective anti-Alzheimer drug candidates, *J. Med. Chem.*, 2008, **51**, 713–716.
11 M.-K. Hu, L.-J. Wu, G. Hsia and M.-H. Yen, Homodimeric Tacrine congeners as acetylcholinesterase inhibitors, *J. Med. Chem.*, 2002, **45**, 2277–2282.
12 https://www.drugs.com/ppa/galantamine.html.
13 P. N. Tariot, P. R. Solomon, J. C. Morris, P. Kershaw, S. Lilienfeld and C. Ding, A 5-month, randomized, placebocontrolled trial of galantamine in AD, *Neurology*, 2000, **54**, 2269–2276.
14 https://www.drugs.com/exelon.html.
15 M. Rösler, R. Anand, A. Cicin-Sain, S. Gauthier, Y. Agid, P. Dal-Bianco, H. B. Stähelin and R. Hartman, Efficacy and safety of rivastigmine in patients with Alzheimer's disease: international randomised controlled trial, *BMJ*, 1999, **318**, 633–640.
16 https://www.drugs.com/mtm/donepezil.html.
17 S. L. Rogers, M. R. Farlow, R. S. Doody, R. Mohs and L. T. Friedhoff, A 24-week, double-blind, placebo-controlled trial of donepezil in patients with Alzheimer's disease, *Neurology*, 1998, **50**, 136–145.
18 M. G. Bursavich, B. A. Harrison and J.-F. Blain, Gamma secretase modulators: new Alzheimer's drugs on the horizon?, *J. Med. Chem.*, 2016, **59**, 7389–7409.
19 G. A. Patani and E. J. LaVoie, Bioisosterism: A Rational Approach in Drug Design, *Chem. Rev.*, 1996, **96**, 3147–3176.
20 G. Zhan, J. Liu, J. Zhou, B. Sun, H. A. Aisa and G. Yao, Amaryllidaceae alkaloids with new framework types from *Zephyranthes candida* as potent acetylcholinesterase inhibitors, *Eur. J. Med. Chem.*, 2017, **127**, 771–780.

21 M. T. Andrade, J. A. Lima, A. C. Pinto, C. M. Rezende, M. P. Carvalho and R. A. Epifanio, Indole alkaloids from *Tabernaemontana australis* (Müell. Arg) Miers that inhibit acetylcholinesterase enzyme, *Bioorg. Med. Chem.*, 2005, **13**, 4092–4095.

22 S. Chigurupati, M. Selvaraj, V. Mani, K. K. Selvarajan, J. I. Mohammad, B. Kaveti, H. Bera, V. R. Palanimuthu, L. K. The and M. Z. Salleh, Identification of novel acetylcholinesterase inhibitors: indolopyrazoline derivatives and molecular docking studies, *Bioorg. Chem.*, 2016, **67**, 9–17.

23 M. Atanasova, G. Stavrakov, I. Philipova, D. Zheleva, N. Yordanov and I. Doytchinova, Galantamine derivatives with indole moiety: docking, design, synthesis and acetylcholinesterase inhibitory activity, *Bioorg. Med. Chem.*, 2015, **23**, 5382–5389.

24 Y. Kia, H. Osman, R. S. Kumar, V. Murugaiyah, A. Basiri, S. Perumal, H. A. Wahab and C. S. Bing, Synthesis and discovery of novel piperidone-grafted mono- and bis-spirooxindole-hexahydropyrrolizines as potent cholinesterase inhibitors, *Bioorg. Med. Chem.*, 2013, **21**, 1696–1707.

25 Y. Kia, H. Osman, R. S. Kumar, V. Murugaiyah, A. Basiri, S. Perumal and I. A. Razak, A facile chemo-, regio- and stereoselective synthesis and cholinesterase inhibitory activity of spirooxindole–pyrrolizine–piperidine hybrids, *Bioorg. Med. Chem. Lett.*, 2013, **23**, 2979–2983.

26 Y. kia, H. Osman, R. S. Kumar, A. Basiri and V. Murugaiyah, Ionic liquid mediated synthesis of mono- and bis-spirooxindole-hexahydropyrrolidines as cholinesterase inhibitors and their molecular docking studies, *Bioorg. Med. Chem.*, 2014, **22**, 1318–1328.

27 Y. Kia, H. Osman, R. S. Kumar, A. Basiri and V. Murugaiyah, Synthesis and discovery of highly functionalized mono- and bis-spiro-pyrrolidines as potent cholinesterase enzyme inhibitors, *Bioorg. Med. Chem. Lett.*, 2014, **24**, 1815–1819.

28 R. F. George, S. S. Panda, E. M. Shalaby, A. M. Srour, I. S. Ahmed Farag and A. S. Girgis, Synthesis and molecular modeling studies of indole-based antitumor agents, *RSC Adv.*, 2016, **6**, 45434–45451.

29 A. S. Girgis, A. F. Mabied, J. Stawinski, L. Hegazy, R. F. George, H. Farag, E. M. Shalaby and I. S. Ahmed Farag, Synthesis and DFT studies of an antitumor active spiro-oxindole, *New J. Chem.*, 2015, **39**, 8017–8027.

30 A. S. Girgis, S. S. Panda, A. M. Srour, H. Farag, N. S. M. Ismail, M. Elgendy, A. K. Abdel-Aziz and A. R. Katritzky, Rational design, synthesis and molecular modeling studies of novel anti-oncological alkaloids against melanoma, *Org. Biomol. Chem.*, 2015, **13**, 6619–6633.

31 L. Yan, W. Yang, L. Li, Y. Shen and Z. Jiang, A one-pot green synthesis of alkylidenesuccinimides, *Chin. J. Chem.*, 2011, **29**, 1906–1910.

32 E. M. Shalaby, A. S. Girgis, H. Farag, A. F. Mabied and A. N. Fitch, Synthesis, X-ray powder diffraction and DFT calculations of vasorelaxant active 3-(arylmethylidene) pyrrolidine-2,5-diones, *RSC Adv.*, 2016, **6**, 112950–112959.

33 A. Kaur, M. Kaur and B. Singh, One-pot regioselective synthesis of novel 1-*N*-methyl-spiro[2,3′]oxindole-spiro [3,3″]-1″-*N*-arylpyrrolidine-2″,5″-dione-4-arylpyrrolidines through multicomponent 1,3-dipolar cycloaddition reaction of azomethine ylide, *J. Heterocycl. Chem.*, 2015, **52**, 827–833.

34 A. S. Girgis, A. F. Mabied, J. Stawinski, L. Hegazy, R. F. George, H. Farag, E. M. Shalaby and I. S. Ahmed Farag, Synthesis and DFT studies of an antitumor active spiro-oxindole, *New J. Chem.*, 2015, **39**, 8017–8027.

35 E. M. Shalaby, A. S. Girgis, A. M. Moustafa, A. M. ElShaabiny, B. E. M. El-Gendy, A. F. Mabied and I. S. Ahmed Farag, Regioselective synthesis, stereochemical structure, spectroscopic characterization and geometry optimization of dispiro[3*H*-indole-3,2′-pyrrolidine-3′,3″-piperidines], *J. Mol. Struct.*, 2014, **1075**, 327–334.

36 I. S. Ahmed Farag, A. S. Girgis, A. A. Ramadan, A. M. Moustafa and A. F. Mabied, 5-Chloro-5″-(4-chlorobenzylidene)-4′-(4-chlorophenyl)-1′,1″-dimethyldispiro[indoline-3,2′-pyrrolidine-3′,3″-piperidine]-2,4″-dione, *Acta Crystallogr., Sect. E: Struct. Rep. Online*, 2014, **70**, o379–o380.

37 N. G. Fawzy, S. S. Panda, W. Fayad, M. A. El-Manawaty, A. M. Srour and A. S. Girgis, Novel curcumin inspired antineoplastic 1-sulfonyl-4-piperidones: design, synthesis and molecular modeling studies, *Anti Canc. Agents Med. Chem.*, 2019, **19**, 1069–1078.

38 S. S. Panda, A. S. Girgis, S. J. Thomas, J. E. Capito, R. F. George, A. Salman, M. A. El-Manawaty and A. Samir, Synthesis, pharmacological profile and 2D-QSAR studies of curcumin-amino acid conjugates as potential drug candidates, *Eur. J. Med. Chem.*, 2020, **196**, 112293.

39 I. A. Seliem, S. S. Panda, A. S. Girgis, Y. I. Nagy, R. F. George, W. Fayad, N. G. Fawzy, T. S. Ibrahim, A. M. M. Al-Mahmoudy, R. Sakhuja and Z. K. M. Abdel-samii, Design, synthesis, antimicrobial and DNA gyrase inhibitory properties of fluoroquinolone-dichloroacetic acid hybrids, *Chem. Biol. Drug Des.*, 2020, **95**, 248–259.

40 N. G. Fawzy, S. S. Panda, W. Fayad, E. M. Shalaby, A. M. Srour and A. S. Girgis, Synthesis, human topoisomerase IIα inhibitory properties and molecular modeling studies of anti-proliferative curcumin mimics, *RSC Adv.*, 2019, **9**, 33761–33774.

41 A. R. Katritzky, A. S. Girgis, S. Slavov, S. R. Tala and I. Stoyanova-Slavova, QSAR modeling, synthesis and bioassay of diverse leukemia RPMI-8226 cell line active agents, *Eur. J. Med. Chem.*, 2010, **45**, 5183–5199.

42 A. M. Srour, D. H. Dawood, M. N. A. Khalil and Z. M. Nofal, Synthesis and 2D-QSAR study of dispiropyrrolodinyl-oxindole based alkaloids as cholinesterase inhibitors, *Bioorg. Chem.*, 2019, **83**, 226–234.

